

# Structural ordering and magnetism in equiatomic CoFeMnSi epitaxial films

Lakhan Bainsla<sup>1</sup>, Resul Yilgin<sup>1</sup>, Jun Okabayashi<sup>2</sup>, Atsuo Ono<sup>1</sup>, Kazuya Suzuki<sup>1</sup> and Shigemi Mizukami<sup>1</sup>

<sup>1</sup> WPI-Advanced Institute for Materials Research, Tohoku Univ.

2-1-1 Katahira, Aoba-ku, Sendai 980-8577, Japan

Phone: +81-2-2217-6004, E-mail: lakhan@tohoku.ac.jp

<sup>2</sup>Research Center for Spectrochemistry, The Univ. of Tokyo, Tokyo, Japan

## Abstract

We report the synthesis and the structural and magnetic properties of CoFeMnSi (CFMS) thin films. Epitaxial films of CFMS are grown on MgO(001) using different post-annealing temperatures ( $T_a$ ). Structural analyses are performed using X-ray diffraction (XRD) measurements at room temperature. The variation in  $L2_1$  and  $B2$  ordering with respect to  $T_a$  is estimated using the XRD measurements by obtaining the (111)/(220) and (002)/(004) intensity ratios, respectively. Gilbert damping constant ( $\alpha$ ) values of  $0.0052 \pm 0.0002$  and  $0.0046 \pm 0.0002$  are obtained for samples with  $T_a = 500$  and  $600^\circ\text{C}$ , respectively, using the ferromagnetic resonance measurements. Element-specific magnetic moment values are obtained using the X-ray magnetic circular dichroism technique. The obtained spin and orbital magnetic moment values suggest a half-metallic ferromagnetic electronic structure with the presence of anti-site chemical disorder. Preliminary measurements on the MTJs show maximum TMR ratio of 70% for the ex-situ annealing of  $450^\circ\text{C}$ .

## 1. Introduction

Half-metallic ferromagnetic (HMF) materials have fully spin polarized band structures and therefore suitable for spintronic applications [1]. Among the large families of HMF materials, Co-based Heusler alloys attracted a lot of attention due to their theoretically predicted half-metallic nature and experimentally observed high spin polarization with high Curie temperatures [1-6]. Equiatomic quaternary Heusler alloys (EQHAs), with Y-type crystal structure are relatively new class of materials and explored very little [7,8]. Depending on the occupation of different lattice sites, there are three types of structural configurations are possible for a Y-type structure [8]. In addition, EQHAs (such as ABCD, where A, B and C are the transition-metal elements and D is a main group element) are prone to possess a various type of chemical disorder. When there is mixing of A and B ( $A=B$ ), the material becomes Heusler-type  $L2_1$  alloy with the composition of  $A_2CD$ . Therefore, when  $A=B$  in an EQHAs, it is referred as a  $L2_1$  ordered system. Another type of possible disorder is C-D disorder, and termed as  $B2$  ordered system. The third type of possible disorder is  $A2$  (bcc) disorder, where all the atoms are randomly distributed. Properties of these materials greatly depend on the chemical ordering in the system. CoFeMnSi (CFMS) is one of the EQHAs, which has been predicted as a spin gapless semiconductor [9,10] and the spin-polarization was relatively high, evaluated by the Point-Contact Andreev Reflection in bulk form [10]. However, there are no reports

available on magnetic tunnel junctions (MTJs) with CFMS thin film electrode. In this study, we investigate the structural and magnetic properties of CFMS epitaxial thin films with tunnel magnetoresistance (TMR) for MTJs.

## 2. Experimental details

30 nm thick CFMS films were grown on single crystalline (001) MgO substrate buffered by 40 nm thick Cr layer using the UHV magnetron sputtering system with a base pressure of less than  $2 \times 10^{-7}$  Pa. Samples with CFMS post-annealed ( $T_a$ ) at 300, 400, 500 and  $600^\circ\text{C}$  were prepared. The composition of the deposited CFMS films was confirmed to be  $\text{Co}_{25}\text{Fe}_{24}\text{Mn}_{24}\text{Si}_{26}$  (at. %) using the inductively coupled plasma (ICP) analysis, which is almost ideal stoichiometric composition for EQHAs.

## 3. Results and discussion

The in-plane XRD patterns show CFMS (200) and (400) peaks for samples with  $T_a \geq 400^\circ\text{C}$  as shown in Fig. 1(a), which indicates that the films are grown with high degree of crystal orientation with respect to MgO (001). Crystallinity of the thin films improves with increase in the  $T_a$ . The respective  $L2_1$  and  $B2$  order parameters for CFMS could be obtained by using the extended Webster model [11]. The respective  $B2$  and  $L2_1$  orders are estimated using the long-range order parameters:

$$S_{B2}^2 = (I_{002} / I_{004}) / (I_{002}^R / I_{004}^R)$$

and

$$(S_{L21}(3 - S_{B2})/2)^2 = (I_{111} / I_{220}) / (I_{111}^R / I_{220}^R),$$

respectively, where  $I_{hkl}$  and  $I_{hkl}^R$  are the experimental X-ray diffraction intensity for (hkl) plane and reference intensity calculated for a fully ordered system, respectively. The estimated order parameters are shown in Fig. 1(b).  $\phi$  scan for (111) and (220) plane was performed by tilting the sample [ $\chi = 54.7^\circ$  for (111) plane and  $\chi = 45^\circ$  for (220) plane], which shows a fourfold symmetry for samples with  $T_a \geq 400^\circ\text{C}$  and thus confirms epitaxial growth of CFMS thin films. In order to get the intensity of CFMS (111) and (220) diffraction peaks,  $2\theta$ - $\theta$  scan was performed with  $\chi=54.7^\circ$  and  $\chi=45^\circ$ . These data indicate that the CFMS films contain the  $B2$  and  $L2_1$  long range orders that change with the  $T_a$ . Because of almost similar scattering factors for Co and Fe, it is virtually impossible to distinguish between Y-type and  $L2_1$  ordering using the  $\text{Cu-K}\alpha$  radiation.

All the films show in-plane magnetic anisotropy. Saturation magnetization ( $M_s$ ) value increases with increase in  $T_a$

and it attains a value of  $590 \text{ emu/cm}^3$  for sample with  $T_a = 600^\circ\text{C}$ . The obtained  $M_s$  value is less than the experimental observed  $M_s$  ( $690 \text{ emu/cm}^3$ ) value for bulk CFMS case [10]. These magnetization data are in accord with x-ray magnetic circular dichroism measurements (XMCD). Coercive field ( $H_C$ ) value also changes with  $T_a$ , and attains  $H_C = 10 \text{ Oe}$  for  $T_a = 600^\circ\text{C}$  sample. Thus, samples with  $T_a \geq 500^\circ\text{C}$  exhibit a soft ferromagnetic behavior similar to other Heusler alloys [2-4,6], therefore they have a high potential for magnetic sensor applications. We emphasize that the samples with high crystallinity represent high  $M_s$  and low  $H_C$  values. Gilbert damping constant values of  $0.0052 \pm 0.0002$  and  $0.0046 \pm 0.0002$  are obtained for samples with  $T_a = 500$  and  $600^\circ\text{C}$ , which is less than the other half-metallic Heusler alloys [12].

Tunneling magneto-resistance effect measurements were performed on the MTJs with optimized growth conditions. The stacking structure of MgO(001) substrate/Cr(40 nm)/CFMS(30 nm)/Mg(0.4 nm)/MgO(1.6 nm)/CoFe(5 nm)/IrMn(10 nm)/Ta(3 nm)/Ru(5 nm) was used for TMR studies. In order to improve the crystallinity of MgO barrier and to obtain exchange bias, MTJs were annealed after the microfabrication in presence of in-plane magnetic field (5 kOe) at different temperatures. TMR was observed with respect to the ex-situ annealing. Preliminary measurements on the MTJs show maximum TMR ratio of 70% for the ex-situ annealing of  $450^\circ\text{C}$ .

#### 4. Summary

Epitaxial growth of the thin films was confirmed from the  $\phi$  scan for (111) and (220) planes, which showed that four-fold structural symmetry for samples with  $T_a \geq 400^\circ\text{C}$ .  $L2_1$  ordering, which was proportional to the (111)/(220) ratio, improves, while  $B2$  ordering, which was proportional to the (002)/(004) intensity ratio, degraded for  $T_a = 600^\circ\text{C}$ . Element-specific magnetic moment values for samples with  $T_a \geq 400^\circ\text{C}$  were obtained using the XMCD measurements at room temperature. Magnetic moment values increased with  $T_a$  similar to the

VSM measurements, and a total magnetic moment value of  $3.38 \mu_B/\text{f.u.}$  is obtained for  $T_a = 600^\circ\text{C}$ . Gilbert damping constant values of  $0.0052 \pm 0.0002$  and  $0.0046 \pm 0.0002$  were obtained for samples with  $T_a = 500$  and  $600^\circ\text{C}$ , which was less than the many other half-metallic Heusler alloys. Therefore, the CFMS material with its unique SGS band structure could be a possible candidate for spintronic applications.

#### Acknowledgements

This work was partially supported by the ImPACT program and Grant-in-Aide for Scientific Research (No. 16K14244).

#### References

- [1] C. Felser, G.H. Fecher, B. Balke, *Angew. Chem. Int. Ed.* 46, (200) 668.
- [2] K. Inomata, N. Ikeda, N. Tezuka, R. Goto, S. Sugimoto, M. Wojcik, E. Jedryka, *Sci. Technol. Adv. Mater* 9, (2008) 014101.
- [3] L. Bainsla, K.G. Suresh, A.K. Nigam, M. Manivel Raja, B.S.D.Ch.S. Varaprasad, Y.K. Takahashi, K. Hono, *J. Appl. Phys.* 116, (2014) 203902.
- [4] H.-X. Liu, Y. Honda, T. Taira, K.-I. Matsuda, M. Arita, T. Uemura, M. Yamamoto, *Appl. Phys. Lett.* 101, (2012) 132418.
- [5] M. Oogane and S. Mizukami, *Phil. Trans. R. Soc. A.* 369, (2011) 3037.
- [6] Y. Sakuraba and K. Takanashi, *Heusler Alloys*. (Eds., Caludia Felser & Atsufumi Hirohata, Springer Series in Materials Science Vol. 222), Chap. 16 (2015) pp. 389-400.
- [7] L. Bainsla and K. G. Suresh, *Applied Physics Reviews* 3, (2016) 031101.
- [8] X. Dai, G. Liu, G.H. Fecher, C. Felser, Y. Li, H. Liu, *J. Appl. Phys.* 105, (2009) 07E901.
- [9] V. Alijani, J. Winterlik, G. H. Fecher, S. S. Naghavi, C. Felser, *Phys. Rev. B* 83, (2011) 184428.
- [10] L. Bainsla, A. I. Mallick, M. Manivel Raja, A. K. Nigam, B.S.D.Ch.S. Varaprasad, Y. K. Takahashi, Aftab Alam, K. G. Suresh, K. Hono, *Phys. Rev. B* 91, (2015) 104408.
- [11] Y. Takamura, R. Nakane, S. Sugahara, *J. Appl. Phys.* 105, (2009) 07B109.
- [12] Lakhan Bainsla, Resul Yilgin, Jun Okabayashi, Atsuo Ono, Kazuya Suzuki, Shigemi Mizukami, submitted, 2017.

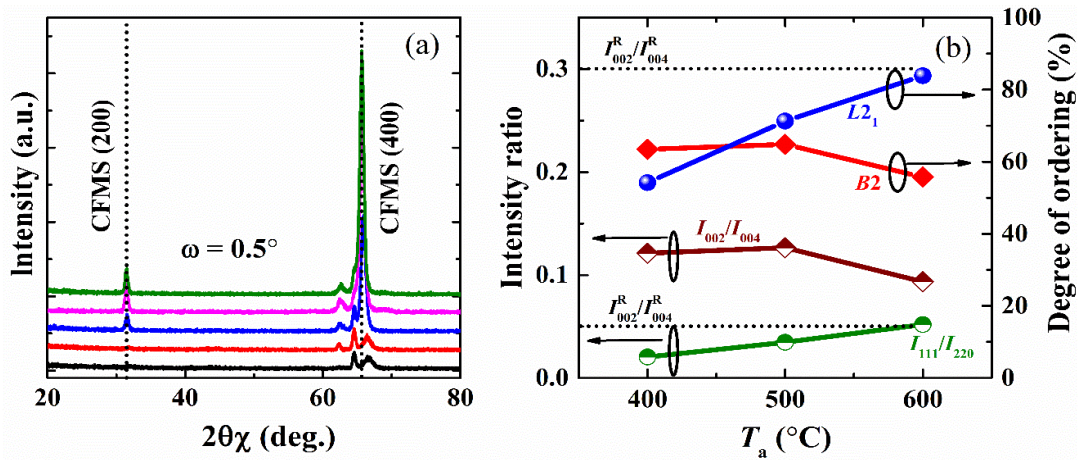


Fig. 1. (a) In-plane XRD measurements. (b) Experimental ( $I_{111}/I_{220}$  and  $I_{002}/I_{004}$ ) and calculated intensity ratios ( $I_{111}^R/I_{220}^R$  and  $I_{002}^R/I_{004}^R$ ) with respect to  $T_a$  are plotted on the left-hand scale, while percentages of ordering parameters are plotted on the right-hand scale.